RSC Advances

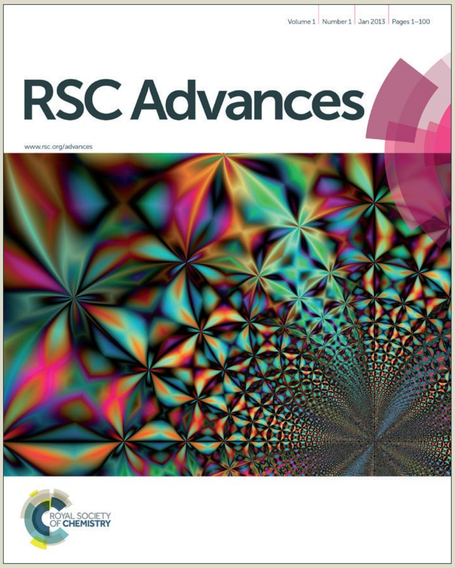

ROYAL SOCIETY OF CHEMISTRY

www.rsc.org/advances

Journal Name

ARTICLE

The Influence of Polyethylene Glycol on the Synthesis and Activity of MoP for the Hydrodechlorination of Trichloroethylene

Received 00th January 20xx,
Accepted 00th January 20xx

DOI: 10.1039/x0xx00000x

www.rsc.org/

Xiaomeng Liu, Lili Ren*

Molybdenum phosphide (MoP), synthesized by combining polyethylene glycol (PEG), shows 4 to 5 times superior activity than the conventional MoP for hydrodechlorination of trichloroethylene (TCE). We investigated the effect of PEG average molecular mass on the catalytic activity of MoP, and found when the average molecular mass of PEG was 8000, MoP catalyst gave the highest activity. Through X-ray diffraction (XRD), N_2 adsorption-desorption, transmission electron microscopy (TEM) and scanning electron microscopy (SEM), H_2 temperature-program reduction (H_2-TPR), the effect of PEG was discussed. The results showed that the addition of PEG changed MoP from original plat structure to lamellar structure, and indeed improved the growth of (101) and (201) crystal planes (the possible crystal plane of high activity) and restrained (100) and (102) crystal planes (the possible crystal plane of low activity). That leads to the high catalytic performance of MoP modified by PEG.

1. Introduction

Recent research has focused on the developments of transition-metal phosphides lying in their potential as catalysts for hydrodesulfurization (HDS) and hydrodenitrogenation (HDN) processes[1-6]. And they showed extremely higher activity than traditional sulfide catalysts, and higher thermal stabilities than metal carbides and nitrides [7, 8].

Molybdenum phosphide (MoP), as a novel hydro-processing catalyst, has received much attention[9-12]. However, transition-mental phosphides usually have relatively low specific surface area[13]. For molybdenum phosphide, its surface area is only about 10 m^2/g[14]. Cheng pointed out that it is difficult to prepare the molybdenum phosphide catalysts with high specific surface area because of the formation of cluster structure during the process of synthesis[15]. Generally, to improve the activity of catalyst efficiently, its surface-to-volume ratio must be maximized. This can be accomplished either by dispersing small catalyst particles on porous supports[16-18] or by using special material to prepare a catalyst with high specific surface area directly[15]. Polyethylene glycol (PEG), as a surfactant, plays a relatively vital role in the synthesis of new material, such as composite material, thin film materials, nano-materials[19-22]. In those cases, polyethylene glycol acted as a structure template or a dispersing agent. In addition, a heterogeneous structure in terms of both size and shape was highly developed and widely distributed with polyethylene glycol[23-27]. And it was found that PEG could improve the catalytic performance of catalyst by modifying the surface structure of the carrier[28, 29].

In this paper, we designed a method by modifying the precursor with polyethylene glycol so as to develop a simple and effective synthesis method for preparing MoP with high catalytic activity. And various analytical techniques have been applied to character the structure of MoP we prepared, including X-ray diffraction (XRD), N_2 adsorption-desorption, H_2 temperature-program reduction (H_2-TPR), transmission electron microscopy (TEM), and scanning electron microscopy (SEM). To evaluate the catalytic activity of the MoP modified by PEG, hydrodechlorination of trichloroethylene (TCE) has been explored as a probe reaction. Trichloroethylene (TCE) is one of the halogenated organic compounds that can be easily found in the emission from chemical processing, ground water and soils due to its extensive uses in industries[30, 31]. Studying on this reaction has a certain guiding role to the rest of the hydrogenation dechlorination reactions and has an important significance for the environment.

2. Experimental

2.1 Preparation of catalyst

The catalyst was prepared according to a method described in the literature[15]. A certain amount of polyethylene glycol (PEG) (Aladdin Industrial Corporation) as a structure agent was added into an aqueous solution containing $(NH_4)_6Mo_7O_{24}\cdot 4H_2O$ (AR, Sinopharm Chemical Reagent Co., Ltd., China) and $(NH_4)_2HPO_4$ (AR, Xilong Chemical Co., Ltd., China). According to the average molecular mass of PEG (1500, 4000, 6000, 8000, 10000), the prepared MoP samples were denoted as MoP-PEG1500, MoP-PEG4000, MoP-PEG6000, MoP-PEG8000, MoP-

---

School of Chemistry & Chemical Engineering, Southeast University, Nanjing, 211189, China.
** E-mail: liliren@seu.edu.cn*

†Electronic Supplementary Information (ESI) available: [Experimental details; Calculation of intensity ratios; Lattice spacing of MoP]. See DOI: 10.1039/x0xx00000x

PEG10000, respectively. The solution was stirred at 353 K for approximately 3 h, and then was dried in a covered beaker in the oil-bath at 373 K. After a further drying at 393K overnight, the sample was calcined at 773 K for 5 h in a fluid air to get the precursor. The precursor was ground with a mortar and pestle, pelletized and sieved to 20-40 mesh. Subsequently, the calcined sample was reduced in H_2 from room temperature to 623 K in 0.5 h and then from 623 K to 923 K at a heating rate of 1 K/min. The sample was reduced at 923 K for 2 h, followed by cooling to room temperature. To prevent the synthesized phosphide upon exposure to air, the sample was passivated in 1% O_2/N_2 for 12 h. Similarly, to compare with the samples above, the MoP in the absence of PEG was prepared by a conventional method, and was denoted as MoP.

2.2 Characterization of materials

XRD patterns were collected on Bruker D8 Discover X-ray diffractometer using Cu *K*α radiation and a nickel filter (λ = 1.5406Å) at a respective voltage of 40 kV and current of 40 mA. The 2*ϑ* scans covered the range of 10º to 80º with a step of 0.02º. N_2 adsorption-desorption measurements were carried out using the conventional multipoint technique with a Belsorp Mini 2. The specific surface areas were calculated according to the Brunauer Emmett Teller (BET) equation while pore distributions were obtained by the Barret-Joyner-Halenda (BJH) method. TEM was carried out on a FEI-G20-2010 electron microscope operated at an acceleration voltage of 200 kV. SEM was performed using a FEI Inspect F50, equipped with an E-T secondary electron detector and an optional back scattering detector.

2.3. Hydrodechlorination (HDC) of trichloroethylene (TCE)

The activities of catalysts for hydrodechlorination have been eagerly studied for the past few years[32-36]. In this catalytic hydrodechlorination, trichloroethylene was reduced using H_2 as the reducing agent in a continuous fixed-bed reactor that contains MoP samples. Before the reactions, the catalysts (volume of catalyst was 4 mL) were reduced at 673 K for 1 h. Using a bubbler for TCE supply, HDC was reacted on the surface of catalyst at different temperatures (400℃, 450℃, 500℃, 550℃, 600℃, 650℃, respectively) in 1 hour. TCE device adopted ice water bath to bring out the same amount by bubbling method. The generated products followed hydrogen into collecting device. The reaction was carried out with gaseous hourly space velocity of 1000 h^{-1}. The flow ratio of H_2 to TCE was adjusted approximately 20:1. The produced HCl was trapped in a water bubbler and the amount of formed HCl can be determined very accurately by NaOH titration with a pH-indicator (e.g. phenolphthalein). The yield coefficient of HCl that reflects the catalyst activity can be calculated to explain the decomposition rate of C-Cl bonds. All experimental data points reported in this paper are the average value of three experiment results.

3. Results and discussion

3.1 Catalytic activity test

To compare the catalytic performance of the MoP using PEG (MoP-PEG) with MoP prepared by the conventional TPR method, the hydrodechlorination of trichloroethylene was studied. Fig.1 shows the C-Cl bonds decomposition rate for hydrodechlorination of TCE over the MoP catalysts at different temperatures. As can be seen in Fig.1, with the rise of temperature, the samples showed nearly same regularity, decrease after the first increases with the maximum conversion at 500 ℃ . However, the MoP-PEG showed obviously higher catalytic performance than the non-modified MoP in general. At 400℃, the conversion of TCE increased from 5.3% to 32.2%. It also shows an absolute advantage over other catalysts that have been reported, 0.5% Pt-$Mg_1Cu_2Al_1$-R catalyst (the conversion of TCE is 30%)[33] and the Pt-CeO_2 catalyst (the highest conversion of TCE is approximately 36%)[34]. We investigate the effect of average molecular mass of PEG on the catalytic activity of MoP. From the Fig.1 we can see that the decomposition of TCE were increasing with the improving average molecular mass of PEG from 1500 to 8000. While when the average molecular mass increased to 10000, the conversion of TCE decreased slightly. MoP-PEG8000 exhibited highest catalytic performance and the conversion of TCE reaches about 75% at 500℃. In conclusion, MoP-PEG indeed improved the catalytic performance in the hydrodechlorination of trichloroethylene reaction and MoP-PEG8000 exhibited the highest catalytic performance in the samples.

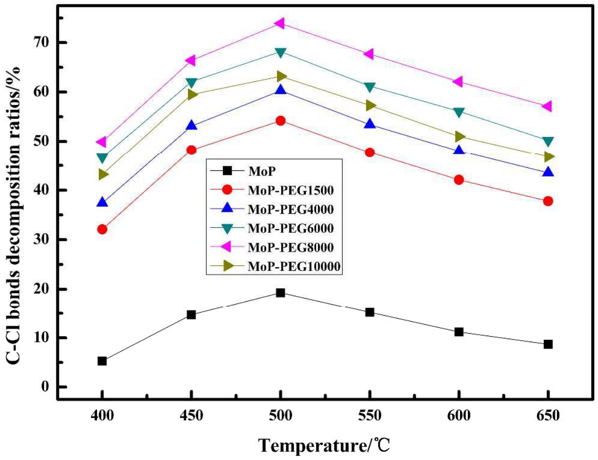

Fig.1 Results of catalysts performed on the hydrodechlorination of trichloroethylene reactions

3.2 Characterization of catalysts

From the above results, the addition of PEG does have a good influence on the catalytic activity. In order to study the effect of PEG on the catalysts, characterization of catalysts have been done as follows.

The BET surface area, pore volume and average pore diameter of the catalyst samples are listed in the Table 1. The surface area for all MoP samples were low (below 15 m^2/g). The results indicate that there was slight change in the specific surface area of the catalyst by using PEG. Accordingly, pore volume and average pore diameter of the catalysts also had a slight change.

Table1. Physicochemical properties of the studied catalysts

Sample	BET surface area (m^2/g)	Pore volume (cm^3/g)	Average pore diameter (nm)
MoP	7.17	0.04716	26.656
MoP-PEG1500	8.787	0.081422	37.065
MoP-PEG4000	9.738	0.0869	29.756
MoP-PEG6000	11.682	0.090835	30.043
MoP-PEG8000	12.094	0.093877	40.041
MoP-PEG10000	8.0494	0.07747	38.497

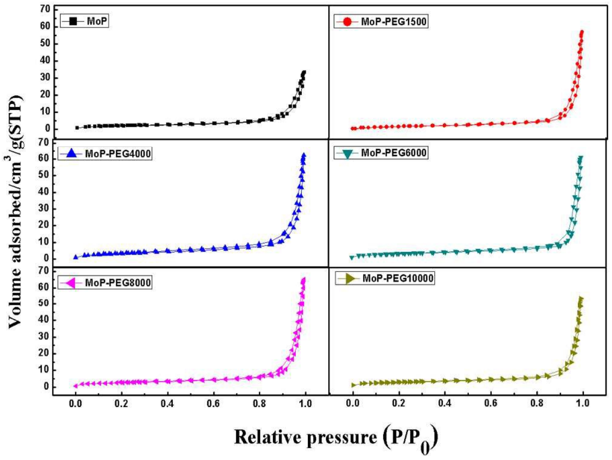

Fig.2 N_2 adsorption-desorption isotherms of catalyst samples

Fig.2 shows the typical N_2 adsorption-desorption isotherms for MoP prepared with different average molecular mass of PEG from 0 to 10000 by TPR method. As can be seen from the Fig.2, MoP shows the lower adsorbed volume than the MoP modified by PEG. The hysteresis loops of the samples prepared with PEG shifted to P/P_0 values at 0.8-1.0 with an increase in the total volume adsorbed, suggesting the possible formation of the cracks through the accumulation of flake particles. What is more, the adsorbed volume changed a little with the increase of average molecular mass from 1500 to 8000 and the volume adsorbed reached the maximum when the average molecule mass of PEG was 8000. For the MoP-PEG10000, the volume adsorbed decreased and the hysteresis loops disappeared, which suggested the formation of cluster structure during the process of synthesis. Combined with Table 1, MoP modified by PEG did get the porous-channel structure so that the porous structure may result in an increase in the catalyst activity. And the formation of porous-channel structure grew with the increasing average molecule mass from 1500 to 8000 so that the catalytic activity improved. However, the overlarge average molecule mass might lead to form cluster structure in the synthesis so that the performance of MoP-PEG10000 decreased. This is consistent with the experimental results. To further explore the reasons of high catalytic activity, we carried out the following characterizations.

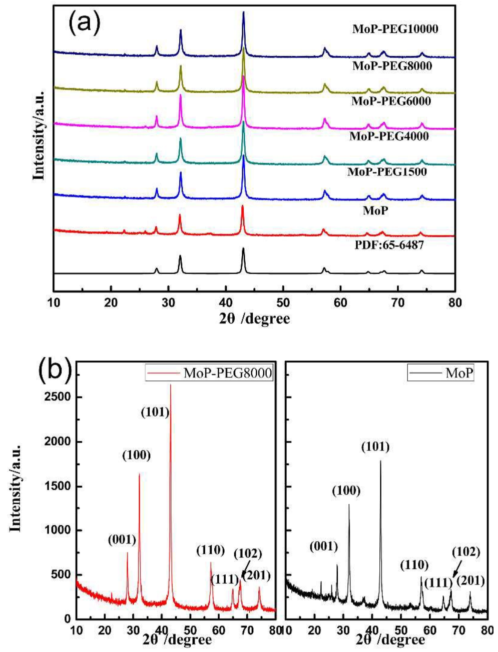

Fig.3 X-ray diffraction patterns of catalyst samples (a) and X-ray diffraction patterns of MoP and MoP-PEG8000 (b)

The XRD patterns in the Fig.3a show the peaks of MoP for all the samples. As can be seen from the Fig.3a, the XRD patterns of MoP samples are well accordance with the standard peak. Fig.3a shows peaks at 28.0º, 32.11º, 43.0º, 57.14º, 64.75º, 68.07ºand 73.95º, which can be attributed to the (001),(100), (101), (110), (111), (102) and (201) crystal planes of the MoP phase (in Fig.3b)[37]. The peak intensities of MoP-PEG8000 are distinctly different from MoP. This suggested that the addition of PEG really changed the nature of the original crystal planes, which made some crystal planes have a stronger response to X-ray than the traditional MoP catalyst. What is more, the size of crystal particles is based on the half-peak width characterization, so sharper diffraction peak shows the bigger particles of crystals. Wang et al.[38] suggested that the preferred orientation can be deduced from the intensity ratio. To deduce the possible preferred orientation, the intensity ratios of different crystal planes were listed in Table 2(the calculation of intensity ratios see in Supporting Information).

Table 2 Intensity ratios of different crystal planes

	$I_{(100)}/I_{(101)}$	$I_{(101)}/I_{(101)}$	$I_{(102)}/I_{(101)}$	$I_{(201)}/I_{(101)}$
PDF-65-6487	69.3	100.0	11.3	14.7
MoP	72.1↑	100.0	17.3	15.7↑
MoP-PEG8000	61.4↓	100.0	17.0	12.7↓

From the $I_{(100)}/I_{(101)}$ ratio, we can find when MoP is modified by PEG, the prepared orientation crystal plane shifts form (100) (low energy crystal plane) to (101) (high energy crystal plane). The different proportion of exposure of a certain crystal plane leads to different catalytic activity[39, 40]. It suggests that the (101) crystal plane is the possible crystal plate of high catalytic activity according to the results of reaction. Accordingly, using PEG retrains the growth of (201) crystal plane because of the lower $I_{(201)}/I_{(101)}$ ratio of MoP-PEG8000. This shows that the (201) crystal plane has little effect on the catalytic activity. In the same way, the $I_{(102)}/I_{(101)}$ ratios of MoP and MoP-PEG8000 are 17.3% and 17.0%. Though the values are same, MoP-PEG8000 is more likely to imply the (102) crystal plane morphology because of the stronger response to the (101) crystal plane. So the (102) crystal plane is also the possible crystal plane of high catalytic activity. The addition of PEG inhibited the growth of the (100) and (201) crystal planes while it promoted the orientation of (101) crystal plane and (102) crystal plane. From what has been discussed above, MoP modified by PEG have superior activity than the traditional MoP because the possible crystal planes of high activity, namely, (101) and (102) crystal planes, grow preferentially while PEG inhibits the growth of (100) and (201) crystal planes.

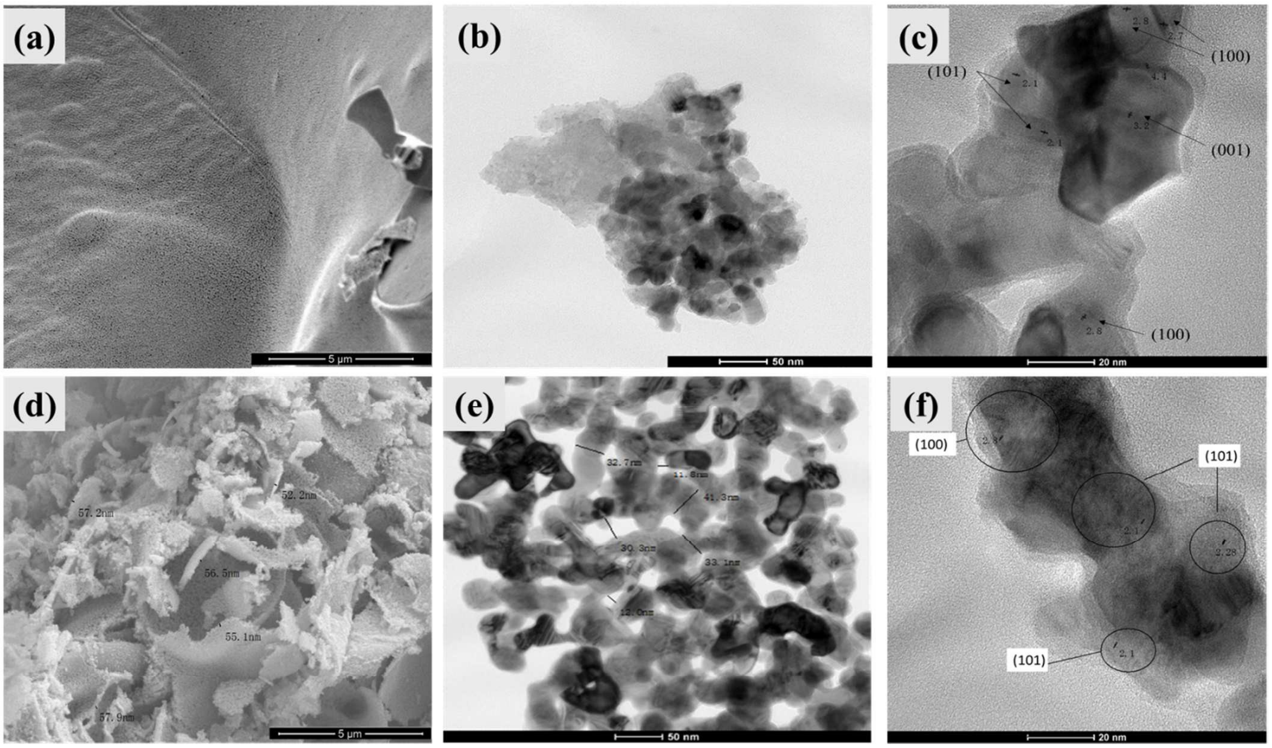

Fig.4 SEM and TEM images of MoP (a, b and c) and MoP-PEG8000 (d, e and f).

Fig.4 shows the morphologies and sizes of MoP and MoP-PEG8000 intermediates investigated by SEM and TEM. It was obvious that they were totally different in morphology and structure. Fig.4a indicates MoP primarily exhibits a flat structure, while disorderly accumulated lamellar structure can be observed in Fig.4d. The energy-dispersion X-ray spectroscope attracted to the SEM analysis of MoP-PEG8000 yielded an elemental composition of 51.61at. % Mo and 48.39 at. % P, which was close to the expected stoichiometric value of 1/1 for MoP. For the MoP, it contained 52.21 and 47.79 at. % of Mo and P, respectively. The TEM images in Fig.4b present the morphologies of MoP, while Fig.4e shows the morphologies of MoP-PEG8000. MoP shows amorphous aggregation of the particles formed the bulk structure, while mesh structure composed of specific worm structure can be seen in Fig.4e. This suggests that MoP-PEG8000 formed the pore structure regularly, which may bring about the exposure of some crystal planes to make diffraction peaks heighten. The

TEM images in Fig.4c and Fig.4f show some crystal planes of MoP and MoP-PEG8000, respectively. Further identification on crystal plane orientation demonstrates that MoP and MoP-PEG8000 have different growth of crystal planes. That is, the exposure facet is mostly (100) for MoP，while crystal growth orientations of (101) are prominent for MoP-PEG8000. The results are superbly consistent with the characterization of XRD. Though (102) crystal plane is absent in Fig.4c and Fig.4f, the orientations of (102) are preferred because of the invariant $I_{(102)}/I_{(101)}$ ratio.

The H_2-TPR profiles of MoP and MoP-PEG8000 precursors are presented in Fig.5. As can be seen in Fig.5, the best reduction temperature of MoP and MoP-PEG8000 precursors are 500℃ and 650℃, respectively. Molybdenum phosphide precursors reduced at 650 ℃ obtained crystal MoP completely[15], and hydrogen consumption peak at 500℃ was caused by reducing from Mo^{6+} to Mo^{4+} [41].The difference of reduction temperature between MoP and MoP-PEG8000 is possibly caused by the different interaction of chemical bonds. The addition of PEG may change chemical interaction to reduce the reduction temperature and the carbonaceous species caused by calcinating PEG might prevent MoP particles from sintering[15]. At the same time, NH_3-TPD had also been carried out (see in the supporting information) in this study. We found that the addition of PEG changed the acid sites (see in Fig.3S). We think adding PEG will change the structure of MoP, which will further lead to the decrease of the reduction temperature and the changes of the acid sites of MoP.

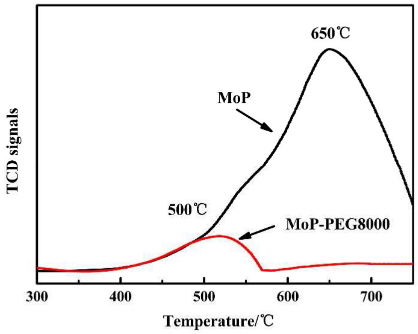

Fig.5 H_2-TPR profiles of MoP and MoP-PEG8000 precursors

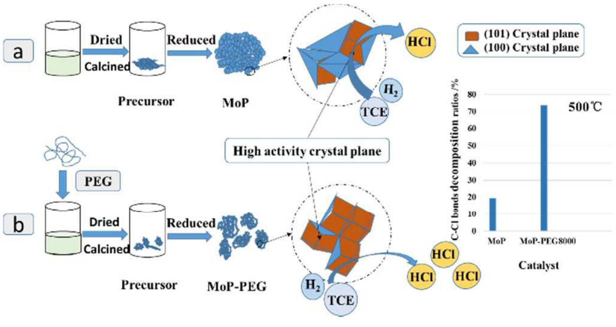

Fig.6 Schematic diagram of (a) MoP (b) MoP-PEG forming and surface reaction

According to the above characterization results, the reaction mechanism can be speculated in Fig.6. As can be seen in Fig.6, traditional preparation of MoP shows cluster of molecule, while MoP modified by PEG exhibits the lamellar structure. The directional structure changed MoP from originally overall aggregation structure to thin plate with porous structure. This was beneficial to expose certain crystal planes which could be the possible crystal planes of high catalytic activity. So the MoP modified by polyethylene glycol showed 4 to 5 times superior activity than the conventional MoP for hydrodechlorination of trichloroethylene. Furthermore, Molybdenum phosphide, modified by different average molecular mass of PEG shows the different TCE conversion ability. This is probably because different average molecular mass of PEG exposed different probability of active crystal planes. However, excessive PEG made molybdenum phosphide reunion which led to a decline in activity.

Conclusions

In conclusion, the addition of PEG changed MoP from original plat structure to lamellar structure, and improved the growth of (101) and (102) crystal planes (the possible crystal plane of high activity) but to restrain (100) and (201) crystal planes (the possible crystal plane of low activity). That leads MoP–PEG to show 4 to 5 times superior activity than the conventional MoP for hydrodechlorination of trichloroethylene. And when the average molecular mass of PEG was 8000, the MoP catalyst showed the highest activity in the reaction.

Acknowledgements

This work was partly financially supported by National Nature Science Foundation of China (21206018), Natural Science Foundation of Jiangsu Province (BK20151408) and the Chinese Funda-mental Research Funds for the Central Universities, (3207045411).

Notes and references

1 S. T. Oyama, Y. K. Lee, *J. Catal.*, 2008, **258**, 393-400.
2 S. Izhar, M. Nagai, *Catal. Today,* 2009, **146**, 172-176.
3 C. A. Montesinos, T. A. Zepeda, B. Pawelec, J. L. G. Fierro and J. A. Reyes, *Chem. Mater.*, 2007, **19**, 5627-5636.
4 A. W. Burns, A. F. Gaudette and M. E. Bussell, *J. Catal.*, 2008, **260**, 262-269.
5 M. A. Infantes, C. Moreno-León and B. Pawelec, *Appl. Catal. B: Environmental*, 2012, **113**, 87-99.
6 A. F. Gaudette, A. W. Burns, J. R. Hayes, M. C. Smith, R. H. Bowker, T. Seda and M. E. Bussell, *J. Catal.,* 2010, **272**, 18-27.
7 S. T. Oyama, *J. Catal.,* 2003, **216**, 343-352.
8 F. Sun, W. Wu and Z. Wu, *J. Catal.*, 2004, **228**, 298-310.
9 C. Stinner, R. Prins and T. Weber, *J. Catal.*, 2000, **191**,438-444.
10 R. Cheng, Y. Shu, M. Zheng, X. Wang, A. Wang and T. Zhang, *J. Catal.*, 2007, **249**, 397-400.
11 M. Nagai, T. Fukiage and S. Kurata, *Catal. Today*, 2005, **106**,201-205.
12 Z. Xing, Q. Liu, A. M. Asiri and X. Sun, *Adv. Mater.*, 2014, **26**, 5702-5707.
13 X. Wang, P. Clark and S. T. Oyama, *J. Catal.*, 2002, **208**, 321-331.

14 W. Li, B. Dhandapani and S. T. Oyama, *Chem. Lett.*, **1998**, 207-208.

15 R. Cheng, Y. Shu, L. Li, M. Zheng, X. Wang, A. Wang and T. Zhang, *Appl. Catal. A: General*, 2007, **316**, 160-168.

16 V. Zuzaniuk, R. Prins, *J. Catal.*, 2003, **219**, 85-96.

17 P. Clark, X. Wang and S. T. Oyama, *J. Catal.*, 2002, **207**, 256-265.

18 Y. Shu, S. T. Oyama, Carbon, 2005, 43, 1517-1532.

19 S. Karaman, A. Karaipekli, A. Sarı, R. Jiraratananon and A. Bicer, *Sol. Energy Mater. Sol. Cells*, 2011, **95**, 1647-1653.

20 S. Wongchitphimon, R. Wang, L. Shi and C. H. Loh, *J. Membr. Sci.*, 2011, **369**, 329-338.

21 M. Yu, S. Huang, K. J. Yu and A. M. Clyne, *Int. J. Mol. Sci.*, 2012, **13**, 5554-5570.

22 J. M. Karp, J. Yeh, G. Eng, J. Fukuda, J. Blumling, K. Y. Suh, J. Cheng and Khademhosseini, A. *Lab. Chip.*, 2007, **7**, 786-794.

23 Z. X. Sun, T. T. Zheng, Q.B. Bo, D. Vaughan and M. Warren, *J. Mater. Chem.*, 2008, **18**, 5941-5947.

24 J. F. Lutz, *J. Polym. Sci Part A: Polym. Chem.*, 2008, **46**, 3459-3470.

25 S. Shamaila, A. K. L. Sajjad, F. Chen and J. Zhang, *Mater. Res. Bull*, 2010, **45**, 1375-1382.

26 T. An, J. Liu, G. Li, S. Zhang, H. Zhao, X. Zeng and J. Fu, *Appl. Catal. A: General*, 2008, **350**, 237-243.

27 F. A. Harraz, S. E. El-Hout, H. M. Killa and I. A. Ibrahim, *J. Catal.*, 2012, **286**, 184-192.

28 S. Onozawa, N. Fukaya, K. Saitou, T. Sakakura and H. Yasuda, *Catal. Lett*, 2011, **141**, 866-871.

29 Z. Hou, N. Theyssen and W. Leitner, *Green Chem.*, 2007, **9**, 127-132.

30 A. Claudia, W. Xiaodong and A.K. Mark, *Chin. J. Catal.*, 2011, **32**, 746-755.

31 O. Orbay, S. Gao, B. Barbaris, E. Rupp, E. Saez, R.G. Arnold and E.A. Betterton, *Appl. Catal. B: Environmental*, 2008, **79**, 7943-7952.

32 Q. Guo, L. Ren, *Catal. Today*, 2015, http://dx.doi.org/10.1016/j.cattod.2015.09.019

33 N. Barrabes, D. Cornado, K. Foettinger, A. Dafinov, J. Llorca, F. Medina and G. Rupprechter, *J. Catal.*, 2009, **263**, 239-246.

34 N. Barrabés, K. Föttinger, A. Dafinov, F. Medina, G. Rupprechter, J. Llorca and J. E. Sueiras, *Appl. Catal. B: Environmental*, 2009, **87**, 84-91.

35 M. Bonarowska, Z. Kaszkur, D. Łomot, M. Rawski and Z. Karpiński, *Appl. Catal. B: Environmental*, 2015, **162**, 45-56.

36 Y. Liu, L. Liu, J. Shan and J. Zhang, *J. Hazard. Mater*, 2015, **290**, 1-8.

37 G Zhou, P. Wang, Z. Jiang and C. Li, *Chin. J. Catal.*, 2011, **32**, 27-30.

38 L. Wang, X. He, W. Sun, L. Wang, Y. Li and S. Fan, *Nano Lett.*, 2012, **12**, 5632-5636.

39 A. Mclaren, T. Valdes-Solis, G. Lin and S. C. Tsang, *J. Am. Chem. Soc.*, 2009, **131**, 12540-12541.

40 E. S. Jang, J. H. Won, S. J. Hwang and J. H. Choy, *Adv. Mater.*, 2006, **18**, 3309-3312.

41 J. Xie, A. Wang and X. Li, *Petro. Processing and Petrochem.*, 2007, **38**, 1-5.

Graphical Abstract